Explaining the Broad-line Region through photoionisation modelling

Swayamtrupta Panda[1·2]

1. Center for Theoretical Physics, Polish Academy of Sciences, Al. Lotników 32/46, 02–668 Warsaw, Poland
2. Nicolaus Copernicus Astronomical Center, Polish Academy of Sciences, Bartycka 18, 00–716 Warsaw, Poland

Broad-line regions (BLR) are one of the main components that constitute the phenomenological picture of active galaxies near the vicinity of the accreting supermassive black holes. Both theoretical and observational studies have shown that the BLR is made of dense, ionized gas clumps that have a strong virialized distribution at parsec-scale distances from the nuclei. Using a theoretically motivated photoionized gas model, I constrain the ionisation parameter (U) and cloud density ($n_{\rm H}$) as a function of the strength of the FeII emission. Recent observations in the reverberation mapping studies have contested the standard radius-luminosity relation, showing increased dispersion in the relation, in particular, after the inclusion of highly accreting quasars. I incorporate the departure coefficient that accounts for this dispersion. This departure term in terms of the dimensionless accretion rate ($\dot{\mathcal{M}}$) and Eddington ratio ($L_{\rm bol}/L_{\rm Edd}$), also includes the virial factor that accounts for the BLR geometry. Then, I combine the fundamental plane relation for the BLR to connect the FeII strength ($\rm R_{FeII}$) in terms of U and $n_{\rm H}$, using selected values for the shape of the broad Hβ profile.

1 Introduction

The Broad-line region (BLR) in the active galaxies (AGN) has been extensively studied from the X-rays to the NIR regime during the last three decades (see the reviews of Sulentic et al., 2000; Gaskell, 2009). One of the most puzzling aspects of the line spectra emitted by the BLR is the FeII emission, whose numerous multiplets form a pseudo-continuum, which extends from the UV to the optical region due to the blending of approximately 10^5 lines. This emission constitutes one of the most important contributors to the cooling of the BLR.

I propose a novel method to combine our existing knowledge about the BLR from both theory and observational standpoints. This analysis will allow us to constrain the $\log U - \log n_{\rm H}$, that is generally used to describe the line emission using photoioization as the fundamental radiation mechanism, in terms of the strength of the FeII, i.e. $\rm R_{FeII}$[1]. Then, I will be able to connect these quantities to (i) the underlying accretion disk (i.e., in terms of the global accretion rate); (ii) a well-represented ionizing continuum for a source accreting about the Eddington limit ($L_{\rm Edd}$); and (iii) combining our knowledge of the BLR cloud composition and geometry. This analytical expression in its final form will be able to describe the BLR with more certainty, wherein observed sources with $\rm R_{FeII}$ measurements can be projected to retrieve the information about the U and $n_{\rm H}$, and vice versa.

---

[1] the integrated flux of the FeII between 4434-4684 Å normalised by the Hβ flux. See Panda et al. (2018) (and references therein) for more details.

The paper is organised as follows. Section 2 derives the $\log U - \log n_{\rm H}$ relation in terms of the $R_{\rm H\beta} - L_{5100}$ relation (Bentz et al., 2013), and subsequently in terms of Eddington ratio ($\lambda_{\rm Edd} = L_{\rm bol}/L_{\rm Edd}$) and black hole mass ($M_{\rm BH}$). The subsequent steps are highlighted briefly in Sec. 2.1.2, which will be addressed in detail in a subsequent paper. The CLOUDY (Ferland et al., 2017) setup for this model is described in Sec. 2.2. Section 3 describes and analyzes one basic scenario of comparing the constant density with the constant pressure model in terms of the FeII, Hβ line emissions, and correspondingly on R$_{\rm FeII}$ in the $\log U - \log n_{\rm H}$ space. I summarize with plans for immediate future work leading into a more comprehensive paper in Sec. 4.

2 Methods and Analysis

2.1 Analytical description

In order to realize the parameter space for the BLR and to link the physical quantities (U,n$_{\rm H}$) and the observable (i.e, R$_{\rm FeII}$), I derive an analytical relation as described in the following sub-sections.

2.1.1 Derivation under $\boldsymbol{R}$-$\boldsymbol{L}_{5100}$ constraint

Starting with the conventional description of the ionization parameter,

$$U = \frac{Q(H)}{4\pi R_{\rm BLR}^2 n_{\rm H} c} = \frac{\Phi(H)}{n_{\rm H} c}, \tag{1}$$

where *Q(H)* is the number of hydrogen-ionizing photons emitted by the central object (in s^{-1}); $R_{\rm BLR}$ is the separation between the central source of ionizing radiation and the inner face of the cloud (in cm); n$_{\rm H}$ is the total hydrogen density (in cm^{-3}); and, $\Phi(H)$ is the surface flux of ionizing photons (in cm^{-2} s^{-1}).

The *Q(H)* term in the above equation can then be replaced with the equivalent *instantaneous* bolometric luminosity ($L_{\rm bol}$),

$$Q(H) = \frac{L_{\rm bol}}{h\nu}. \tag{2}$$

This bolometric luminosity can then be replaced with a crude assumption, i.e. $L_{\rm bol} = A \times {\rm L}_{5100}$, where A is the bolometric correction (see Netzer, 2019, for a recent review). This gives us the relation,

$$\log U = \log\left(\frac{A{\rm L}_{5100}}{h\nu_{5100} \times 4\pi R_{\rm BLR}^2 n_{\rm H} c}\right). \tag{3}$$

From the *Clean2* sample of Bentz et al. (2013), we have,

$$\log\left(\frac{R_{\rm BLR}}{1\ light - day}\right) = \kappa + \alpha \log\left(\frac{{\rm L}_\lambda}{10^{44}}\right). \tag{4}$$

Substituting Eq.4 in Eq.3, we have

$$\begin{aligned}\log U =& \log\left[\frac{A}{4\pi h\nu_\lambda (1\ light - day)^2 c}\right] - 2(\kappa - 44\alpha)\\ &+ [(1-2\alpha)\log {\rm L}_\lambda] - \log n_{\rm H}.\end{aligned} \tag{5}$$

Here, the used values for κ and α are 1.555 and 0.5 (instead of the quoted value of 0.542), respectively. Also, I assume an average value for A = 9 (Richards et al., 2006; Elvis et al., 1994). I get a simplified relation between U and $\mathrm{n_H}$,

$$\log U = B - \log n_{\mathrm{H}}. \tag{6}$$

Here, the value of B = $10.85\bar{1}$, where B is

$$B = \log\left(\frac{A}{4\pi h\nu_{5100} c}\right) - 2\kappa + \log 10^{44} - 2\log(1\ light - day). \tag{7}$$

2.1.2 In terms of λ_{Edd} and M_{BH}

Interpreting this in terms of *Eddington ratio*, λ_{Edd}

$$\log U = C - \log n_H + (1-2\alpha)\log\left[\lambda_{\mathrm{Edd}} L_{\mathrm{Edd}}\right], \tag{8}$$

where

$$C = B - (1-2\alpha)\log A. \tag{9}$$

Equation 8 can then be re-written in terms of black-hole mass, M_{BH}

$$\boxed{\log U = D - \log n_{\mathrm{H}} + (1-2\alpha)\log\left[\lambda_{\mathrm{Edd}} M_{\mathrm{BH}}\right]}, \tag{10}$$

where

$$D = C + (1-2\alpha)\log\left(\frac{4\pi G \mathrm{M}_{\odot} m_{\mathrm{p}} c}{\sigma_{\mathrm{T}}}\right), \tag{11}$$

where M_{BH} is measured in units of solar mass ($\mathrm{M}_{\odot}$); G is the Gravitational constant; m_{p} is the mass of a proton (in cgs); σ_{T} is the Thompson's cross-section (in cgs).

In Panda et al. (in prep.), we combine this knowledge with two other key entities – (a) the departure coefficient $\Delta R_{\mathrm{H}\beta}$ (Martínez-Aldama et al., 2019); and (b) the BLR fundamental plane relation (Du et al., 2016). Eventually, I have an analytical expression that combines the BLR picture from the physical point of view, i.e., using the ionization parameter (U) and cloud density (n_{H}), and, to the observational perspective, $\mathrm{R_{FeII}}$ and $L_{\mathrm{bol}}/L_{\mathrm{Edd}}$. This will also include the dependence on the shape of the Hβ line profile and the effect of the viewing angle.

2.2 CLOUDY simulations

Taking inspiration from the Locally Optimally Emitting Clouds (LOC) model (Baldwin et al., 1995), I perform a suite of models by varying the cloud particle density, n_{H}, and the ionization parameter, U. The model assumes a distribution of cloud densities at various radii from the central illuminating source to mimic the gas distribution around the close vicinity of the active nuclei. Although, I extract directly the emission line information from each of the single cloud models and do not integrate the line emission from the clouds. The remaining parameters are the cloud column density (N_{H}), for which we incorporate a value of 10^{24} cm^{-2}, motivated by our past studies (Panda et al., 2017, 2018, 2019a). Indeed, one expects a broad range of column densities to be present in the BLR, yet, this value of the N_{H} quite consistently reproduces the observed line emission, especially in the case of the optical and UV FeII as is shown in Bruhweiler & Verner (2008). I use solar abundance which was estimated using the *GASS10* module (Grevesse et al., 2010).

We utilize the spectral energy distribution for the nearby (z= 0.0611) Narrow Line Seyfert 1 (NLS1), *I Zwicky 1* (hereafter I Zw 1) also known as PG 0050+124 or Mrk 1502. The I Zw 1 ionizing continuum shape is obtained from VizeR[2]. I Zw 1 is a prototypical optical NLS1, with strong FeII emission and unusually narrow permitted lines, e.g. Hβ FWHM 1240 $\mathrm{km\,s^{-1}}$ (Osterbrock & Pogge, 1985), and it is also a luminous radio-quiet PG QSO ($\mathrm{M_B}$=-23.5, Schmidt & Green 1983). The bolometric luminosity of I Zw 1 is $\mathrm{L_{bol}} \sim 3\times10^{45}$ erg $\mathrm{s^{-1}}$ (Porquet et al., 2004), which for a black hole mass of $2.8^{+0.6}_{-0.7}\times10^{7}$ $\mathrm{M_\odot}$ (Vestergaard & Peterson, 2006) implies that, I Zw 1 accretes at a rate close to the Eddington limit. The parameter $\mathrm{R_{FeII}}$ is extracted from these simulations.

3 Results and Discussions

It has been shown in previous studies (Adhikari et al., 2018) that there is a substantial change in the gas pressure profile and correspondingly the density profiles, when models with constant density and constant pressure are compared side-by-side. The profiles are almost in-line for lower densities i.e., $n_\mathrm{H} \lesssim 10^9$ $\mathrm{cm^{-3}}$. But, the profiles start to diverge for $n_\mathrm{H} \gtrsim 10^9$ $\mathrm{cm^{-3}}$ and then substantially becomes wider. Thus, for dense clouds ($n_\mathrm{H} \gtrsim 10^{10}$ $\mathrm{cm^{-3}}$), constant pressure and constant density models give very similar $\mathrm{R_{FeII}}$ estimates.

In the context of the current work, I show this difference in a more extended $\log U - \log n_\mathrm{H}$ parameter space, and comparing the two models side-by-side (Fig. 1, 2 and 3). The results shown in both panels in Fig. 1, 2 and 3 are without the effect of dust. This effect will be presented and analyzed in an upcoming paper. The density maps clearly show multiple peaks in the $\mathrm{R_{FeII}}$ values as a function of changing $\log U$ and $\log n_\mathrm{H}$, especially the three peaks – (Region A) short region about the (-6.5,8); (Region B) the elongated region in the middle spanning from (-6,13) to (0,5); and (Region C) third patch that extends from (-4.5,13) to (-1,9). Taking hint from various previous works, the effective BLR densities have been found to span between $\sim 10^9$–10^{12} (in $\mathrm{cm^{-3}}$) or even higher in some cases (Ilić et al., 2012; Baskin et al., 2014; Marziani et al., 2015; Czerny, 2019). Additionally, in the ionisation parameter context, very high values imply that the BLR clouds can be maximally ionized, and this will lead to suppression of various line emission. This will not only quench the observed emission from HILs, but also for the LILs, such as the Hβ and the FeII emission observed in the optical band. Thus, the region A and almost whole of the region B gets omitted based on these reasoning. In Panda et al. (in prep.), we show that with the inclusion of dust (applying realistic dust temperature prescription from Nenkova et al. 2008) we are finally left with the region C which best describes the BLR in AGNs.

4 Conclusions and Future

I derive an analytical expression that will seamlessly tie together the fundamental BLR properties coming from theory and observations. This relation combines the

---

[2] http://vizier.u-strasbg.fr/vizier/sed/

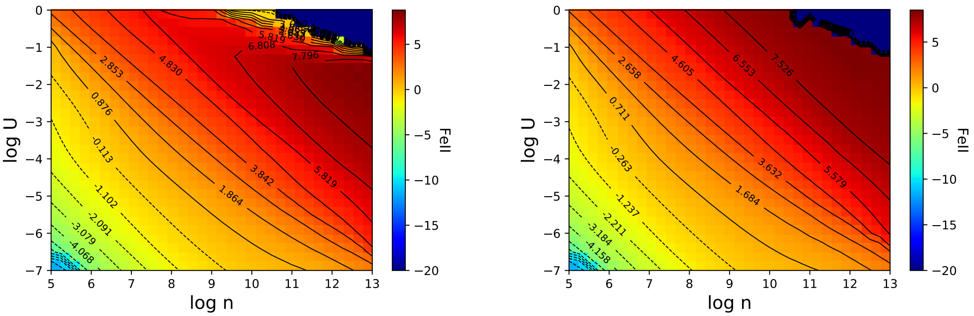

Fig. 1: 2D histograms showing $\log U - \log n_{\rm H}$ for FeII for (a) constant density; (b) constant pressure. The model uses solar abundance ($Z_\odot$) and 0 $\rm km\,s^{-1}$ microturbulence.

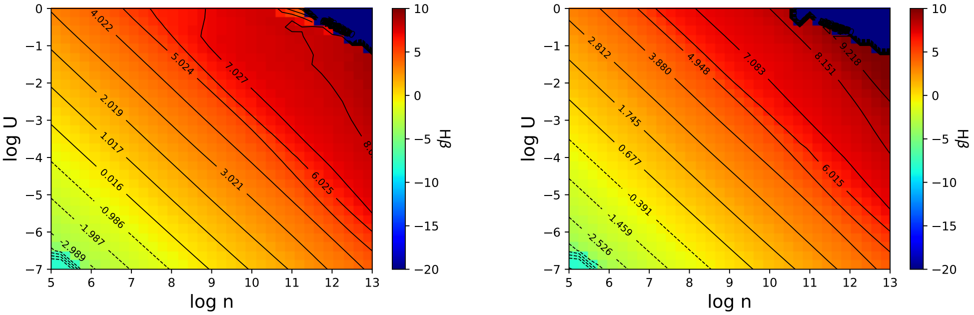

Fig. 2: 2D histograms showing $\log U - \log n_{\rm H}$ for Hβ for (a) constant density; (b) constant pressure. The model uses solar abundance ($Z_\odot$) and 0 $\rm km\,s^{-1}$ microturbulence.

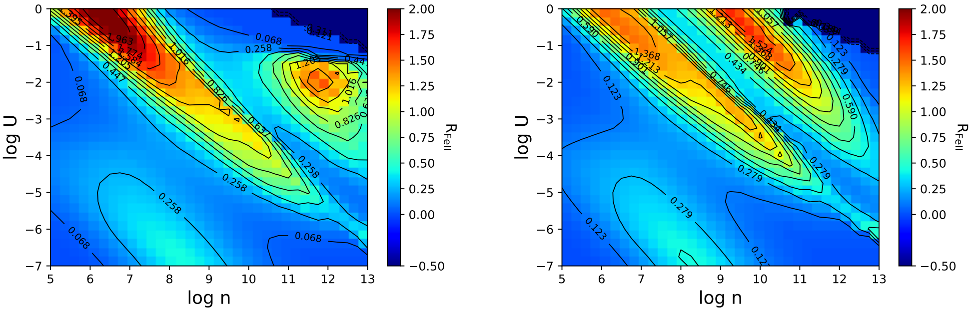

Fig. 3: 2D histograms showing $\log U - \log n_{\rm H}$ for $\rm R_{FeII}$ for (a) constant density; (b) constant pressure. The model uses solar abundance ($Z_\odot$) and 0 $\rm km\,s^{-1}$ microturbulence.

$\log U - \log n_{\rm H}$ relation from the photoionization theory with the observationally constrained relations, such as the $R_{\rm H\beta} - L_{5100}$ (and others as described in Sec. 2.1.2), in terms of the Eigenvector 1 parameter, $\rm R_{FeII}$ (for more details see Panda et al., 2018, 2019a, 2020, 2019b). I have shown preliminary results from a suite of models using CLOUDY photoionization code. These results will be further expanded and tested for (i) the effect of dust inclusion at larger depths within the BLR clouds; (ii) the effect of changing the ionizing continua; and (iii) changing chemical composition and dynamics within the cloud.

Acknowledgements. The project was partially supported by National Science Centre, Poland, grant No. 2017/26/A/ST9/00756 (Maestro 9). I would like to thank Bożena Czerny, Mary Loli Martínez Aldama, Paola Marziani, Deepika Ananda Bollimpalli and Abbas Askar for fruitful discussions leading to this project.

References

Adhikari, T. P., et al., *ApJ* **856**, 78 (2018)

Baldwin, J., Ferland, G., Korista, K., Verner, D., *ApJ* **455**, L119 (1995)

Baskin, A., Laor, A., Stern, J., *MNRAS* **438**, 604 (2014)

Bentz, M. C., et al., *ApJ* **767**, 149 (2013)

Bruhweiler, F., Verner, E., *ApJ* **675**, 83-95 (2008)

Czerny, B., *Open Astronomy* **28**, 1, 200 (2019)

Du, P., et al., *ApJ* **818**, L14 (2016)

Elvis, M., et al., *ApJS* **95**, 1 (1994)

Ferland, G. J., et al., *Rev. Mexicana Astron. Astrofis.* **53**, 385 (2017)

Gaskell, C. M., *New A Rev.* **53**, 7-10, 140 (2009)

Grevesse, N., Asplund, M., Sauval, A. J., Scott, P., *Ap&SS* **328**, 179 (2010)

Ilić, D., et al., *A&A* **543**, A142 (2012)

Martínez-Aldama, M. L., et al., *ApJ* **883**, 2, 170 (2019)

Marziani, P., et al., *ApSS* **356**, 339 (2015)

Nenkova, M., Sirocky, M. M., Ivezić, Ž., Elitzur, M., *ApJ* **685**, 1, 147 (2008)

Netzer, H., *MNRAS* **488**, 4, 5185 (2019)

Osterbrock, D. E., Pogge, R. W., *ApJ* **297**, 166 (1985)

Panda, S., Czerny, B., Done, C., Kubota, A., *ApJ* **875**, 133 (2019a)

Panda, S., Czerny, B., Wildy, C., *Frontiers in Astronomy and Space Sciences* **4**, 33 (2017)

Panda, S., Marziani, P., Czerny, B., *ApJ* **882**, 2, 79 (2019b)

Panda, S., Marziani, P., Czerny, B., *Contributions of the Astronomical Observatory Skalnate Pleso* **50**, 1, 293 (2020)

Panda, S., et al., *ApJ* **866**, 115 (2018)

Porquet, D., Reeves, J. N., O'Brien, P., Brinkmann, W., *A&A* **422**, 85 (2004)

Richards, G. T., et al., *ApJS* **166**, 470 (2006)

Schmidt, M., Green, R. F., *ApJ* **269**, 352 (1983)

Sulentic, J. W., Marziani, P., Dultzin-Hacyan, D., *ARA&A* **38**, 521 (2000)

Vestergaard, M., Peterson, B. M., *ApJ* **641**, 2, 689 (2006)